JOM, Vol. 66, No. 4, 2014
DOI: 10.1007/s11837-014-0922-2

Processing for Highly Emissive CZ-Silicon by Depositing Stressed Sol–Gel Films

S. ABEDRABBO,[1,2,3] A.T. FIORY,[2] and N.M. RAVINDRA[2]

1.—Department of Physics, The University of Jordan, Amman 11942, Jordan. 2.—Department of Physics, New Jersey Institute of Technology, Newark, NJ 07901, USA. 3.—e-mail: sxa0215@yahoo.com

Enhanced band-gap emission from Czochralski silicon substrates of up to ~100 times is reported. This was achieved by processing for a stressed interface resulting from baked and annealed silica films prepared by sol–gel processes. The active dopants include but are not limited to erbium and are prepared with tetraethylorthosilicate (TEOS) while forming the active precursors using oxide and nitrate forms of the rare earth. In addition, annealed films produce infrared emission in the 1.5-μm band from erbium ions in the film. Steady-state photoluminescence studies indicate that a strong correlation of the intensity of the emission at the band gap to the stress formed at the interface and is a direct function of the annealing temperature of the silica films, independent from the known erbium 4*f* emission bands.

INTRODUCTION

Spin-coating of sol–gel films is widely applied as a cost-effective process for depositing nominally pure and impurity-doped thin silica films on substrates (see Ref. 1). Of interest are optically active coatings suitable for silicon-integrated optoelectronics. The present method entails depositing erbium-doped silica films on silicon wafer material that is densified by thermal annealing. With suitable selection of thermal annealing temperature (T_a), photoluminescence (PL) measurements show strong emission in the 1.5-μm wavelength band from Er^{+3} centers in silica (Stark-split intra-4*f* $4I_{13/2}$–$4I_{15/2}$ transitions of Er^{+3})[2] for $T_a \approx 850°C$;[3] additionally, near band-gap emission at 1.16 μm from the silicon becomes greatly enhanced for $T_a \approx 700°C$.[4] Section "Optical Emission From Erbium" describes the experimental procedures and reports on the analysis of PL from Er^{+3} in the sol–gel material. Section "Enhanced Optical Emission From Silicon" presents analysis of PL from the silicon. General conclusions are presented in section "Conclusions".

OPTICAL EMISSION FROM ERBIUM

Optical telecommunication networks use rare-earth doped optical materials for a variety of applications, e.g., fiber and waveguide amplifiers, waveguides by index of refraction modification, infrared (IR) light sources, integrated optical devices, and displays and lasers,[2,5–8] and silica doped with erbium is a widely used optical material. Although SiO_2:Er can be prepared in film form by a variety of methods, spin-coating of sol–gels acquired special interest because of low deposition temperature and low overall cost.[6,7,9–13] For this work, a sol–gel technique was developed using Er_2O_3 as the Er dopant source and introduced at high concentration (6 at.%) in the SiO_2:Er film. The process yields optically active erbium-doped silica films at moderate annealing temperatures ($T_a \sim 850°C$). An example of a suitable optoelectronic application is in fabrication of planar erbium-doped waveguide amplifiers (EDWAs).

Erbium Sol–Gel Processing

The erbium-doped sol was produced by hydrolysis of tetraethylorthosilicate (TEOS, $Si(OC_2H_5)_4$) in a solution containing erbium oxide and then annealing the gel. The relatively high Er concentration of 6 at.% is expected to form stable Er-O:Si-O structures, owing to the strong Er-O bond (6.3 eV[14]) and the role of Er as a network element in glasses.[15,16] Special considerations of sol–gel processes concern quenching of the 1.5-μm emission by resonant energy

(Published online March 18, 2014)

transfer to vibrations of residual OH[1,17] and dependence of external emission on Er concentration.[10,11] Much residual OH can be removed with high-temperature annealing (e.g., T_a ~900–1100°C [8,18]); however, T_a <1000°C is preferable for integrated silicon-based optoelectronics and glass reflow processing.[19] In the process developed for the present work, T_a ~850°C turns out to be sufficient for removing the effects of residual OH as well as for reducing surface pores area to maintain a low level of OH, thereby avoiding high-temperature processing.

Experimental Procedure

The starting solution for the sol–gel process contained 0.5 g Er_2O_3 powder mixed into a solution of 4-mL ethanol, 4-mL acetic acid, and 1.6-mL deionized water that was stirred at 45°C for 3 h. The sol was then prepared by the addition of 2-mL TEOS and stirring for 10 min at 80°C. Hydrolysis with high water/TEOS molar ratio R (here, R = 10) with acid catalysis produces branched Si-O polymerization in the sol and leads to dense films;[20] the trade-off is an increased hydroxyl content to be removed by thermal annealing.[13] After this step, the solution was passed through a syringe filter with 0.45-μm pore size and spun coated on 2.5-cm pieces of cleaned Si (100) wafer substrates rotating at 1200 rpm for 30 s. The resulting gel films were then oven dried in air at 120°C for 30 min. Postdeposition thermal treatment was studied by vacuum annealing (2 Pa) at temperatures (T_a) spanning the range 500–950°C for a duration of 1 h (t_{anneal}). Prior work has shown that vacuum annealing is more effective in removing OH contaminants than annealing in air, as determined from an increased Er^{+3} emission lifetime.[13]

Film thickness and index of refraction were determined using a thin-film spectrophotometer. A model Fluorolog-3 spectrofluorometer (Horiba Jobin–Yvon, Edison, NJ) was used to obtain room-temperature PL emission from the Er^{+3} centers in the 1535-nm band. A Xe lamp was used for excitation with a double excitation monochromator to set a fixed excitation wavelength in the range of 515–530 nm. Spectral signal intensities were recorded in the range 1400–1600 nm using a LN cooled Hamamatsu InGaAs photodiode detector, preceded by a single-emission monochromator, using 0.2 s of integration time at each wavelength. Emission from Er^{+3} in the 1535-nm band was maximized by tuning the excitation monochrometer to 521–523 nm, as obtained from a three-dimensional matrix of PL-excitation spectra. PL spectra were normalized to the power output of the excitation source, monitored by a separate photodiode.

Annealing is generally required to densify sol–gel films by removing water, organic compounds, and hydroxyl residues;[8,18] most volatiles are driven off at T_a ~500°C.[10] Films may densify by ~25%, which is observed in this work as shrinkage in thickness

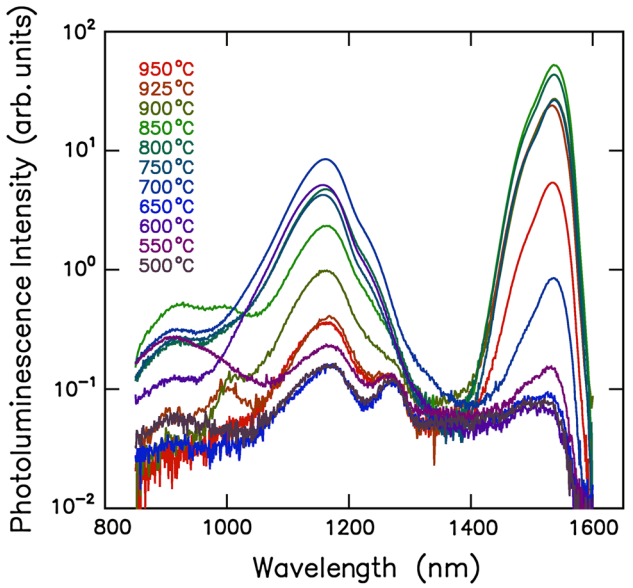

Fig. 1. PL intensity spectra from silicon coated with erbium-doped sol–gel silica films (anneal temperatures T_a in legend) (Color figure online).

from ~170 nm (air-dried) to ~130 nm (T_a ~700°C). The T_a for producing the strongest PL depends on the process method as well as on the Er concentration (e.g., T_a ~900°C are often used for sol–gel films[6,7,21]). Decreased emission at high annealing temperatures can arise from several causes: Segregation by precipitation of Er or phase separation by clustering, and quenching by Er-Er interactions at high optically active Er^{+3} concentrations, as well as residual OH contamination.[22]

Results: Erbium Emission

PL spectra for samples annealed at various T_a are presented in Fig. 1 (normalized logarithmic intensity scale). Peaks near 1160 nm originate from the silicon substrate (see section "Enhanced Optical Emission From Silicon"), while emission peaks near 1535 nm arise from Er^{+3} in the sol–gel film. Erbium emission from the as-deposited air-dried sample is very weak and hardly noticed when compared with annealed samples. This is to be expected because low-temperature baking leaves residues from the sol and an abundance of water and hydroxyls in a low-density porous near-glassy network. As such it is expected that nonradiative recombination strongly competes with the radiative ones, leading to the low PL signal observed.

The PL signal from the Er^{+3} appreciably improves as a function of increasing T_a, particularly for T_a >700°C, until it reaches a maximum at T_a ≈850°C. Samples annealed at higher T_a exhibit a decreasing trend in their PL (confirmed out to 1050°C for additionally prepared samples annealed in either air or vacuum). Maximum PL intensity occurs at emission wavelengths in the vicinity of 1533–

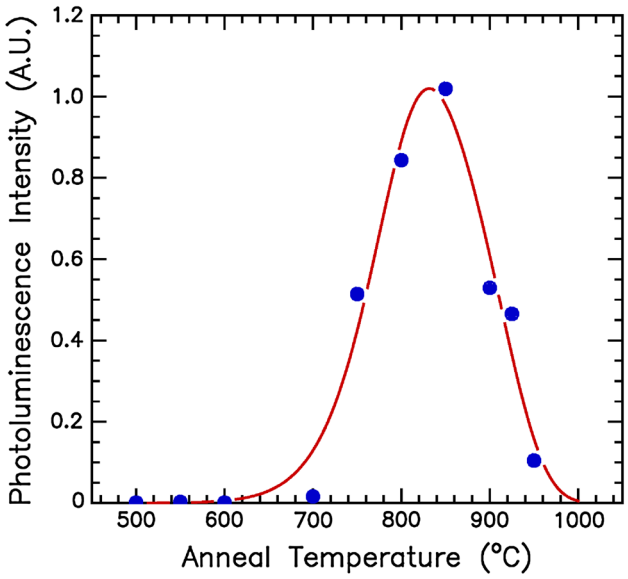

Fig. 2. Maximum Er^{+3} PL intensities (~1535 nm) from silicon coated with erbium-doped sol–gel silica films versus anneal temperature (data: points; theory: curve).

1537 nm, and spectral full width at half maximum is in the range 51–58 nm, both varying somewhat with T_a. To illustrate the trend, peak PL intensities (normalized arbitrary units; integrated spectra are similar) are plotted against T_a in Fig. 2 as filled circles (uncertainties for anneals above 600°C are ~12% full scale). The evident non-monotonic dependence on T_a is indicative of competing thermal reactions that activate optical emission from the intra 4*f* Er^{+3} band as T_a is increased toward 850°C, and deactivate it at the higher T_a.

In Ref., 3 a model involving two activation energies was introduced to provide a quantitative analysis of the dependence of the PL from the Er on T_a. An energy E_a is defined as the activation energy of the favorable process (forming optically active Er^{+3}), and an energy E_d is defined as the activation energy of the unfavorable process (quenching optically active Er^{+3}). Fitting the model to the data yields the results $E_a = 2.3 \pm 0.6$ eV and $E_d = 2.6 \pm 0.7$ eV, and the theoretical function shown in Fig. 2; error bars in the activation energies arise from parameter correlation and uncertainty in the data. The magnitude of the activation energies is consistent with the idea that OH removal is the mechanism by which the otherwise optically active Er^{+3} yields the PL signal. Interpretations of these results will be discussed.

Influence of Hydroxyl on Er^{+3} Emission

The presence of OH is extremely effective in quenching excited Er^{+3} ions.[17] At high OH concentrations, direct resonant energy transfer from the excited ion to OH serves as an extremely effective trap. At low OH concentrations, fast transfer of energy from ion to ion via the Förster mechanism (cooperative energy transfer or CET) may allow diffusion of the excitation to an OH impurity, where it becomes dissipated by multi-phonon-assisted decay to the oxide host.[23] The latter process is a type of concentration quenching because the rare-earth concentration is the dominant factor in the CET coefficient.[22] In the present case, both mechanisms are expected to apply because the Er concentration is quite high.

Weak PL emission for the low-temperature anneals ($T_a \ll 850$°C) indicates quenching of excited Er^{+3} ions by direct Er $\rightarrow$ OH interactions. Increase in PL intensity in the region $T_a \leq 850$°C is therefore consistent with removing OH from proximity to Er^{+3} ions. Residual OH is mostly surface bonded within pores in the form of silanol groups, as shown by IR absorption near 3670 cm^{-1} observed in bulk silica gels (~900°C anneals).[24,25] An identified mechanism for OH removal is surface desorption of H_2O, which is released upon reaction of surface silanol to form siloxane bridge structures, corresponding to an enthalpy $\Delta H = 2.16$ eV.[26] (Bulk studies indicate OH diffuses very rapidly at 850°C.[27]) Because $E_a \approx \Delta H$ within error, one may associate creation of optically active Er^{+3} with the process of OH removal by desorption.

As the observed diminution of PL intensity at higher annealing temperatures corresponds to a thermal activation energy E_d that is also on the order of that for OH processes, it appears that OH removal is involved in the PL deactivation as well. Reduced concentrations of residual OH obtained for high-temperature annealing may allow the diffusive Er $\rightarrow$ Er $\rightarrow$ OH processes to become effective for quenching PL emission. Moreover, high Er concentration in itself (e.g., upon virtually eliminating OH and densifying as Er-Er distances decrease) can lead to concentration quenching by cross relaxation or cooperative upconversion processes (CUPs) involving Er-Er dipolar interactions, a form of CET, that typically converts one out of two units of excitation energy into heat; this CUP mechanism has been reported for optical fibers with high Er concentrations.[28] Both of these mechanisms can account for the decrease in PL emission for annealing in the region $850\text{°C} \ll T_a \leq 1050$°C.

Diffusivity of Er at low concentrations in various deposited silica films was recently measured in the temperature range 1000–1100°C,[29] from which an activation energy $E_{Er} = 5.3$ eV was derived, due mainly to strong Er-O bonds, which are also responsible for the stability of Er-glass structures; extrapolation to 950°C yields diffusivity $D_{Er} \approx 6 \times 10^{-17}$ cm^2 s^{-1} and diffusion length $(4D_{Er}\, t_{anneal})^{1/2} \sim 10$ nm. Erbium diffusion therefore appears to be sufficient for Er clustering at 950°C, owing to the high Er concentration in the sol–gel films (mean Er-Er distance ~1 nm); Er clustering generally kills the optical activity of the involved Er ions. Although Er segregation may participate along the other mechanisms

leading to overall PL quenching for T_a post 850°C, Er is considered a primary network component at comparable concentrations[15] favoring a stable Si-O-Er glassy network.

As in fiber amplifiers doped with Er at high concentration, one expects the Er-Er interaction to saturate the PL but not to shrink it. However, as sol–gel films are usually not completely densified and Er diffusion is negligible for anneals near 850°C, CET is minimized for T_a ~850°C while OH out-diffusion is very welcomed. Higher annealing temperature permits the Er-Er interaction to occur at a much higher rate due to a faster densification process where PL deterioration can be spurred by anyone or more of the briefed processes.

These results are quite different from the concentration quenching observed at low Er concentrations. The existence of a range in annealing temperatures where concentration quenching may appear suppressed is a particular advantage obtained by using a high Er concentration. One does not expect thermal annealing behavior to materially depend on Er concentration because the optimal anneal temperature depends mainly the OH concentration that dominates the process. The optimum T_a at 6 at.% Er is somewhat lower than previously reported for sol–gel films with less than 1 at.% Er;[6,7,21] this is similar to the behavior of Er-doped silicon-rich oxides, where optimal T_a is lowered by about 100°C at Er concentrations of 3–6 at.%.[30]

ENHANCED OPTICAL EMISSION FROM SILICON

The PL spectra of Fig. 1 shows emission at 1.067 eV (1162 nm), which is just below the Si band gap (energy units used herein by convention). Analysis presented below shows that this room-temperature emission from silicon is enhanced by the Er-doped sol–gel coatings and is correlated with inhomogeneous film stresses. Obtaining high efficiency in light emission from silicon at room temperature has traditionally entailed selecting structures and materials to circumvent inherent disadvantages of the indirect Si band gap (e.g., typical 10^{-4} quantum efficiency (QE) at 300 K;[31] see also Ref. 32).[33] Thus, this sol–gel process method has inherent advantages as a simplified process.

Results: Enhanced Silicon Emission

PL spectra are shown in Fig. 3 for two samples that were annealed at T_a of 700°C and 850°C (solid and broken curves, respectively) and exhibit major peaks at 0.807 eV and 1.067 eV. The 1.067-eV peak is strongest for annealing at 700°C, where it is enhanced by a factor of 50 when compared with unannealed, air-dried films; as verified below, emission at 1.067 eV is associated with the Si substrate.

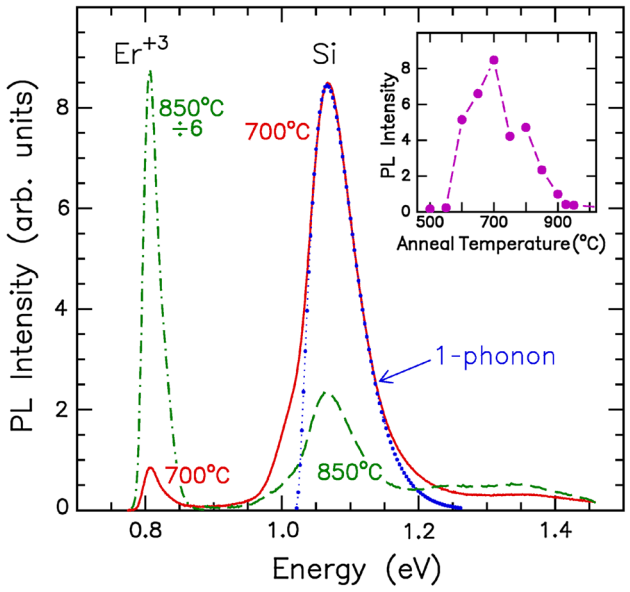

Fig. 3. PL intensity spectra for two silicon coated with erbium-doped sol–gel silica films, annealed at 700°C (Si: solid curve) and 850°C (Er^{+3}: dashed; chain-dashed, scaled by 6). Dotted curve denotes one-phonon theory. Insert: peak PL from Si (~1.067 eV) versus anneal temperature.

The 0.807-eV peak is strongest for annealing at 850°C (left dot-dash curve reduced by factor of 6) and is associated with emission from Er^{+3} in the silica film, as discussed in section "Optical Emission From Erbium". Weaker emissions in the region 1.25–1.35 eV are attributed to $^4I_{11/2} \rightarrow {}^4I_{15/2}$ transitions in Er^{+3}. Annealing at T_a = 850°C corresponds to maximum 0.807-eV Er^{+3} emission. On comparing the two emission signals, the peak emission from the Si (T_a = 700°C) is about 16% of the peak emission from Er^{+3} (T_a = 850°C); from areas under the respective spectra, the integrated signal from the Si is 50% of that from Er^{+3}.

The dotted curve in Fig. 3 is a theoretical one-phonon (i.e., dominant phonon) model for emission of photons at energy E by phonon-assisted recombination of free electrons and holes in silicon, represented by the expression, $PL(E) \propto (E - E_0)^2 \exp[-(E - E_0)/k_BT$ (uncorrelated pair model, see Ref. 34); it is calculated with threshold energy E_0 = 1.020 eV and thermal energy k_BT = 0.023 eV. Owing to this function, the PL spectra generally exhibit exponential tails for $E > E_0$. As the dominant phonons are the momentum-conserving transverse optical phonons of energy E_{ph} = 0.0578 eV, the effective band gap, neglecting possible corrections for exciton binding or trapping, is $E_G = E_0 + E_{ph}$ = 1.078 eV, which is about 42 meV below the intrinsic Si band gap (1.12 eV). This is an approximate examination of the data as the effect of weaker phonon components, e.g., features appearing below 1.03 eV, were not included; the reasonable overlap for much of the PL signal peaking at

1.067 eV indicates that this emission originates indeed from the silicon substrate and not the film. X-ray diffraction data show no evidence of polycrystalline Si (e.g., absence of Si nanocrystals within the deposited film[33]).

Annealing behavior for emission from Er^{+3} in the sol–gel film and from the Si substrate obey distinctly different dependences on T_a (compare Figs. 2 and 3, inset). This qualitatively shows that emission from the Si is not directly related to the Er^{+3} ions in the silica film, from which we conclude that emissions at these two wavelengths arise from independent mechanisms.

Influence of Sol–Gel Coating on Si Emission

The observed annealing behavior points to enhancement of emission from the silicon arising from a reversible (owing to non-monotonic dependence on T_a) interaction with the sol–gel coating. Stresses in sol–gel films, caused by shrinkage and porosity, are known to be inhomogeneous as indicated by IR absorption signatures (frequency shifted TO_3 modes at 1060–1080 cm^{-1}),[35] and tend to be greatest for T_a ~700°C,[36] which coincidentally is where the strongest Si PL from our samples is observed. Given that Si PL is comparatively subdued for T_a <600°C as well as for T_a >900°C, one may conclude that enhanced PL at T_a ~700°C is to be associated with nonuniformities in film stresses.

Inhomogeneous film stresses, acting in concert with native interfacial roughness, is therefore expected to create local strain-induced band bending in the silicon and increase the effective cross section for radiative free-carrier recombination. Applying this interpretation, enhanced emission is expected to be produced in only a thin layer at the Si surface (on the order of the film thickness, ~0.1 μm, or less); because the excitation radiation penetrates ~1 μm, QE could actually be increased a thousand-fold (i.e., on the order of ten times larger than the observed enhancement), suggesting QE >1% (assuming QE ≤0.01% as reported for Czochralski (CZ) silicon[31,32]).

CONCLUSIONS

A process for producing optically active SiO_2:Er thin films on Si substrates using low-cost sol–gel techniques that use Er_2O_3 has been presented and analyzed. PL is enhanced strongly as a function of annealing temperature, reaching optimum for annealing temperatures in a 50°C range near 850°C. External emission from Er-O structures is shielded by OH for annealing temperatures T_a < 850°C and by the combination of Er concentration quenching and Er-Er-OH energy diffusion for T_a > 850°C. The results indicate that minima in quenching by Er-Er CET and by Er-OH interactions can be associated with T_a ≈ 850°C.

In addition, near-band-gap (1.067 eV) PL at room temperature has been observed in CZ Si wafer material with the erbium-doped sol–gel silica coating. Emission from the Si, strongest for T_a ≈700°C, correlates with inhomogeneous stresses in sol–gel films (owing to strong 25% shrinkage), as indicated indirectly from IR absorption. Based on the independent annealing behavior of the two PL signals and comparison with prior studies of sol–gel film properties, it appears that the Er is not directly involved in the Si emission. The spin-coating process presented herein is notable for enhancing light emission from bulk-type Si (estimated QE ~1%) in the absence of any patterning or *p–n* junctions.

ACKNOWLEDGEMENTS

Support offered by The University of Jordan and the Deanship of Academic Research the University are gratefully acknowledged. The authors would like to acknowledge the support of Bashar Lahlouh of The University of Jordan and Sudhakar Shet previously from the National Renewable Energy Laboratory for their valuable assistance.

REFERENCES

1. M. Ferrari, Processing, Characterization, and Applications.*Handbook of Sol–Gel Science and Technology*, Vol. II, ed. S. Sakka (Norwell: Klewer Academic Publishers/ Springer, 2005), pp. 359–389.
2. E. Desurvire, *Erbium Doped Fiber Amplifiers: Principles and Applications* (New York, NY: Wiley, 1994), pp. 207–305.
3. S. Abedrabbo, B. Lahlouh, and A.T. Fiory, *J. Phys. D* 44, 315401 (2011).
4. S. Abedrabbo, B. Lahlouh, S. Shet, and A.T. Fiory, *Scr. Mater.* 65, 767 (2011).
5. Q. Wang, N.K. Dutta, and R. Ahrens, *J. Appl. Phys.* 95, 4025 (2004).
6. G.C. Righini, S. Pelli, M. Ferrari, C. Armellini, L. Zampedri, C. Tosello, S. Ronchin, R. Rolli, E. Moser, M. Montagna, A. Chiasera, and S.J.L. Ribeiro, *Opt. Quant. Electron.* 34, 1151 (2002).
7. X. Orignac, D. Barbier, X.M. Du, R.M. Almeida, O. McCarthy, and E. Yeatman, *Opt. Mater.* 12, 1 (1999).
8. Q. Xiang, Y. Zhou, B.S. Ooi, Y.L. Lam, Y.C. Chan, and C.H. Kam, *Thin Solid Films* 370, 243 (2000).
9. Y.Y. Hui, P.-H. Shih, K.-J. Sun, and C.-F. Lin, *Thin Solid Films* 515, 6754 (2007).
10. C.K. Ryu, H. Choi, and K. Kim, *Appl. Phys. Lett.* 66, 2496 (1995).
11. X. Orignac, D. Barbier, X.M. Du, and R.M. Almeida, *Appl. Phys. Lett.* 69, 895 (1996).
12. L.H. Slooff, M.J.A. de Dood, A. van Blaaderen, and A. Polman, *Appl. Phys. Lett.* 76, 3682 (2000).
13. L.H. Slooff, M.J.A. de Dood, A. van Blaaderen, and A. Polman, *J Non-Cryst Solids* 296, 158 (2001).
14. K.P. Huber and G. Herzberg, *Molecular Spectra and Molecular Structure IV. Constants Diatomic Molecules* (New York, NY: Van Nostrand Reinhold, 1979), p. 212.
15. J.T. Kohli and J.E. Shelby, *Phys. Chem. Glasses* 32, 67 (1991).
16. J.E. Shelby and J.T. Kohli, *J. Am. Ceram. Soc.* 73, 39 (1990).
17. A.J. Bruce, W.A. Reed, A.E. Neeves, L.R. Copeland, and W.H. Grodkiewicz, *Proceedings of the Optical Waveguide Materials—Materials Research Soceity*, (Pittsburgh, PA: MRS, 1992), pp. 157–161.
18. S. Pal, A. Mandal, G. De, E. Trave, V. Bello, G. Mattei, P. Mazzoldi, and C. Sada, *J. Appl. Phys.* 108, 113116 (2010).
19. S. Wolf, *Silicon Processing for the VLSI Era, Process Technology*, 2nd ed., Vol. 2 (Sunset Beach, CA: Lattice Press, 2000).

20. C.J. Brinker and G.W. Scherer, *J. Non-Cryst. Solids* 70, 301 (1985).
21. A.C. Marques, R.M. Almeida, A. Chiasera, and M. Ferrari, *J. Non-Cryst. Solids* 322, 272 (2003).
22. A. Polman, *Physica B* 300, 78 (2001).
23. V.P. Gapontsev, S.M. Matitsin, A.A. Isineev, and V.B. Kravchenko, *Opt. Laser Technol.* 14, 189 (1982).
24. S. Kondo, F. Fujiwara, and M. Muroya, *J. Colloid Interface Sci.* 55, 421 (1976).
25. J.H. Anderson Jr and K.A. Wickersheim, *Surf. Sci.* 2, 25 (1964).
26. C.J. Brinker, G.W. Scherer, and E.P. Roth, *J. Non-Cryst. Solids* 72, 345 (1985).
27. K.M. Davis and M. Tomozawa, *J. Non-Cryst. Solids* 185, 203 (1995).
28. R. Wyatt, *Fiber Laser Sources and Amplifiers (Proceedings of SPIE)*, Vol. 1171, ed. M.J.F. Digonnet (Bellingham, WA: SPIE, 1989), pp. 55–64.
29. Y.-W. Lu, B. Julsgaard, M.C. Petersen, R.V.S. Jensen, T.G. Pedersen, K. Pedersen, and A.N. Larsen, *Appl. Phys. Lett.* 97, 141903 (2010).
30. G.W. Adeola, H. Rinnert, P. Miska, and M. Vergnat, *J. Appl. Phys.* 102, 053515 (2007).
31. D.J. Lockwood, *Light Emission in Silicon: From Physics to Devices, Semiconductors and Semimetals Series*, ed. D.J. Lockwood (Chestnut Hill, MA: Academic Press, 1998), pp. 1–35.
32. O. King and D.G. Hall, *Phys. Rev. B* 50, 10661 (1994).
33. L. Pavesi and D. Lockwood, *Silicon Photonics, Topics in Applied Physics*, Vol. 94 (Berlin, Germany: Springer, 2004).
34. G. Weiser, S. Kazitsyna-Baranovski, and R. Stangl, *J. Mater. Sci.* 18, S93 (2007).
35. P. Innocenzi, *J. Non-Cryst. Solids* 316, 309 (2003).
36. T.M. Parrill, *J. Mater. Res.* 9, 723 (1994).